

Article

Enhanced Leaching of Zinc from Zinc-Containing Metallurgical Residues via Microwave Calcium Activation Pretreatment

Aiyuan Ma ^{1,2}, Xuemei Zheng ^{1,2}, Lei Gao ^{3,4}, Kangqiang Li ^{3,4,5,*}, Mamdouh Omran ^{6,7,*}  and Guo Chen ^{3,4,*}

¹ School of Chemistry and Materials Engineering, Liupanshui Normal University, Liupanshui 553004, China; may_kmust11@163.com (A.M.); zxm_lpssy19@163.com (X.Z.)

² Guizhou Provincial Key Laboratory of Coal Clean Utilisation, Liupanshui 553004, China

³ Kunming Key Laboratory of Energy Materials Chemistry, Yunnan Minzu University, Kunming 650500, China; glkust2013@hotmail.com

⁴ Key Laboratory of Green-Chemistry Materials, University of Yunnan Province, Kunming 650106, China

⁵ Key Laboratory of Aerospace Materials and Performance, Ministry of Education, School of Materials Science and Engineering, Beihang University, Beijing 100191, China

⁶ Process Metallurgy Research Group, Faculty of Technology, University of Oulu, 90014 Oulu, Finland

⁷ Central Metallurgical Research and Development Institute (CMRDI), Cairo 11421, Egypt

* Correspondence: kqlikust@126.com (K.L.); mamdouh.omran@oulu.fi (M.O.); guochen@kust.edu (G.C.)

Abstract: Given the shortage of zinc resource, the low utilisation efficiency of secondary zinc resource, and the crucial problem that the synchronous dissolution of zinc from different mineral phases, an activation pretreatment method merged with calcium activation and microwave heating approach was proposed to enhance the zinc leaching from complex encapsulated zinc-containing metallurgical residues (ZMR). Results indicated that under the optimal pretreatment conditions, including microwave activation temperature of 400 °C, CaO addition of 25% and activation time of 20 min, the zinc leaching rate reached 91.67%, which was 3.9% higher than that by conventional roasting pretreatment. Meanwhile, microwave heating presents excellent treatment effects, manifested by the zinc leaching rates, all exceeding that of conventional roasting under the same conditions, while the process temperature is decreased by 200 °C. In addition, XRD and SEM-EDS analysis denoted that microwave calcification pretreatment can effectively promote the transformation of the refractory zinc minerals like Zn₂SiO₄ and ZnFe₂O₄ into the easily leachable zinc oxides. The distinctive selective heating characteristics of microwave heating strengthened the dissociation of mineral inclusion, and the generated cracks increased the interfacial reaction area and further enhancing the leaching reaction of zinc from ZMR.

Keywords: zinc-containing metallurgical residues; calcium activation; microwave heating; enhanced leaching



Citation: Ma, A.; Zheng, X.; Gao, L.; Li, K.; Omran, M.; Chen, G. Enhanced Leaching of Zinc from Zinc-Containing Metallurgical Residues via Microwave Calcium Activation Pretreatment. *Metals* **2021**, *11*, 1922. <https://doi.org/10.3390/met11121922>

Academic Editor: Jean François Blais

Received: 26 October 2021

Accepted: 19 November 2021

Published: 28 November 2021

Publisher's Note: MDPI stays neutral with regard to jurisdictional claims in published maps and institutional affiliations.



Copyright: © 2021 by the authors. Licensee MDPI, Basel, Switzerland. This article is an open access article distributed under the terms and conditions of the Creative Commons Attribution (CC BY) license (<https://creativecommons.org/licenses/by/4.0/>).

1. Introduction

Zinc (Zn) is a key transition metal with excellent wear resistance, calenderability, and corrosion resistance; thereby its applications involve anticorrosive galvanised sheet, alloy materials, battery materials, and non-ferrous metallurgy [1,2]. Currently, zinc sulphide ores is the main ore for zinc production. As the demand for Zn-based materials increases, zinc sulphide resources are gradually depleted, and its grade is getting lower and lower, which severely hinders industrial production [3,4]. The output of hazardous metallurgical residues is also considerable and needs to be treated efficiently. Therefore, it is urgent and of significant and sound research value to exploit and utilise the secondary zinc resource, zinc-containing metallurgical residues (ZMR). These residues are usually accompanied with the production of iron, zinc and lead. The iron and steel industry produces many kinds of ZMR, such as blast furnace dust, converter dust, electric arc furnace dust and other dust [5]. When producing 1 ton of crude steel, approximately 15–20 kg/ton of electric arc furnace dust is produced, and the amount of electric arc furnace dust is increasing with

the increase in steel output [6]. The zinc content in dust is about 10~25%, with significant recovery value [7]. Besides, the lead-zinc smelting industry also generates a large amount of slag containing about 10~20% of zinc [8], and this slag also confers numerous toxic compositions such as chromium, cadmium, and arsenic [9]. If ZMR is directly stacked without treatment, it will cause land occupation, environmental pollution and waste of zinc resources [10]. Therefore, it is important to recover Zn from ZMR for resource recycling and environmental protection [11].

The Zn recovery from ZMR is difficult due to the complex phases, high gangue and serious pelletization of ZMR [12]. Zinc in ZMR always presents as multi-phase, like ZnCO_3 , ZnS , Zn_2SiO_4 , and ZnFe_2O_4 . Meanwhile, it also contains the impurities of gangues (silica and aluminium), halogens (fluorine and chlorine), lead, iron, and cadmium [3]. Currently, many processes are proposed for recycling Zn from ZMR, such as pyrometallurgical and hydrometallurgical methods [13]. The pyrometallurgical process relies on carbon as a heating agent and reducing agent. However, it suffers from strict reduction conditions, high energy consumption, large investment, and huge harmful gas emissions [14]. It is also unsuitable for processing low-grade zinc sources. Hydrometallurgical treatment with low energy consumption has attracted wide attention and exploration to treat ZMR. Since zinc oxide is an amphoteric oxide which can be dissolved in an acid or alkali solution, the appropriate leaching agent can be selected to separate zinc and other impurities. At present, the mature technologies mainly involve acid leaching, alkali leaching, and ammonia leaching, accompanying its respective advantages and disadvantages [15]. During the acid leaching, the lower acid concentration and oxidizing media can inhibit and reduce the iron dissolution [16], hence only ZnO phase can be effectively extracted. Thus, the total leaching efficiency of zinc is very low under lower acid concentration [17]. Conversely, the higher acid concentration is needed to extract zinc from zinc ferrite, but zinc silicate and zinc sulfide cannot be extracted, except from in the circumstance of sulfuric acid with oxidizing media [18]. Meanwhile, the higher acid concentration will cause the alkaline gangue to enter the solution, further blocking the pipeline; and silicon components will react in acid to form silica gel, further rendering the filtration difficult. Furthermore, the fluorine and chlorine will enter into the acidic solution and affect the quality of zinc in the electrowinning process [19]. Regarding alkali leaching, lower equipment requirements are needed and better selectivity can be achieved, compared to acid leaching. However, its overall cost is higher, and roasting pretreatment is needed before alkali leaching [20]. Furthermore, using NaOH as leaching agent, silica and lead will dissolve with Zn in solution; hence, the leaching solution needs to purify before the final electrowinning process [21]. Generally speaking, the feasibility of the industrial application of alkali leaching method is low. Furthermore, in ammonium leaching method, zinc oxide and zinc carbonate can form soluble complexes with ammonium agent in the leaching solution; meanwhile, iron, carbon, fluorine and chlorine components, and basic gangue (such as aluminium and silicon) remain in the solid residue [22,23]. The addition of $\text{CH}_3\text{COONH}_4$ into the $\text{NH}_3\text{-H}_2\text{O}$ solution can promote the conversion of the $[\text{Zn}(\text{NH}_3)_4]^{2+}$ compounds into the more stable compounds, significantly improving the Zn leaching efficiency via a more economical and environmental way [24]. The mixture solution of $\text{CH}_3\text{COONH}_4$ and $\text{NH}_3\text{-H}_2\text{O}$ is verified to be the most effective leaching agent for recovering Zn from ZMR [24]. However, the Zn leaching efficiency is still low when Zn in ZMR exists in the phases of zinc ferrite or zinc silicate, attributed to these phases are stable and difficult to dissolve in ammonium solution [25].

Calcium activation with adding CaO to pretreat ZMR may have some contribution to solving the above problems bothering the ammonium leaching method. It refers to that ZnFe_2O_4 will react with CaO at 900–1100 °C, and convert to ZnO and $\text{Ca}_2\text{Fe}_2\text{O}_5$ without carbothermic reduction, further improving the Zn leaching efficiency [15,26]. Meanwhile, CaO activation pretreatment also has the advantage of removing fluoride, chloride, and heavy metals without resulting in the necessary evaporation loss of zinc and iron [15]. However, the process temperature and time of this conventional treatment both need

to be reduced to decrease energy cost. In contrast to conventional heating, microwave heating endows the distinctive advantages of shorter time and lower process temperature, selective heating, and controllable operation [27–34]. Due to the difference of microwave absorption of various useful minerals and gangue minerals, different heating efficiencies will appear during microwave heating. The ores will generate cracks by the thermal stress, which will promote the dissociation of useful mineral monomers and improve the recovery of target metals [35–39]. Therefore, microwaves can be used as an alternative energy source of conventional heating to process ZMR in a more energy-saving and environmental protection approach [40–42].

The previous study reported the respective utilisation of CaO activation pretreatment [15,26] or microwave heating [29,30] to process metallurgical residues and highlighted the two ways that are effective for improving the Zn leaching efficiency [15,26,29,30]. However, no detailed study has reported processing zinc-containing metallurgical residues (ZMR) with the two ways merged, even the leaching mechanism of ZMR by the combined approach. Therefore, the present study proposed a new hybrid process to enhance the Zn leaching from ZMR, wherein the ZMR was roasted by microwave activation pretreatment with the addition of CaO, followed by the roasted ZMR sample were leached in $\text{NH}_3\text{-CH}_3\text{COONH}_4\text{-H}_2\text{O}$ solution. The effects of CaO addition, microwave activation temperature, and activation time on the Zn leaching efficiency were investigated and optimised. Meanwhile, the advantages of the new process were evaluated by comparing conventional roasting treatment. Furthermore, laser particle size analyser, scanning electron microscopy (SEM), energy dispersive spectroscopy (EDS), and X-ray diffraction (XRD) were employed to analyse the mechanism of this pretreatment.

2. Experimental

2.1. Materials

The raw material of zinc-containing metallurgical residues (ZMR) was derived from a secondary zinc resource recovery industry (Kunming, Yunnan, China), which is a mixture of various types of metallurgical slag and dust (MSD). The ZMR sample contains the zinc-containing gas mud (ash) produced in the blast furnace smelting process, the zinc-containing dust produced in the electric arc furnace smelting process. In addition to soot, there are parts of the zinc-containing smoke and dust after the volatilization of the lead smelting slag in the lead-zinc smelting process and the leaching slag in the hydro-zinc smelting process. Table 1 illustrates the chemical composition of the raw material. As presented in Table 1, the raw material has a complex composition with the high contents like zinc of 24.74% and iron of 21.66%. Besides, it also contains the rare metal indium (In) with a content of about 354 g/t, and a high content of chlorine (Cl) and plenty of basic gangue components. In summary, the residues could be determined with high recycling value.

Table 1. Chemical compositions of the ZMR sample.

Chemical Composition						
Compositions Content (w%)	Zn 24.74	Fe 21.66	C 9.14	Pb 1.13	Mg 1.14	Al_2O_3 2.22
Compositions Content (w%)	CaO 4.10	Cl 2.94	Si 2.66	S 1.39	Bi 0.97	In 0.035

Figure 1 displays the XRD pattern and particle size distribution of the raw ZMR. It is concluded that zinc mainly presents in the forms of ZnO, ZnS, Zn_2SiO_4 , ZnFe_2O_4 , and $\text{Zn}_5(\text{OH})_8\text{Cl}_2 \cdot \text{H}_2\text{O}$, while iron presents in Fe_3O_4 and Fe_2O_3 , and the complicated phase compositions render the Zn recycling process more difficult. According to the previous research, ZnS, Zn_2SiO_4 , and ZnFe_2O_4 are refractory mineral phases in $\text{NH}_3\text{-CH}_3\text{COONH}_4\text{-H}_2\text{O}$ solution [22]. To further improve the Zn leaching efficiency, it is necessary to pretreat these refractory mineral phases to transform them into the easily leachable mineral phases.

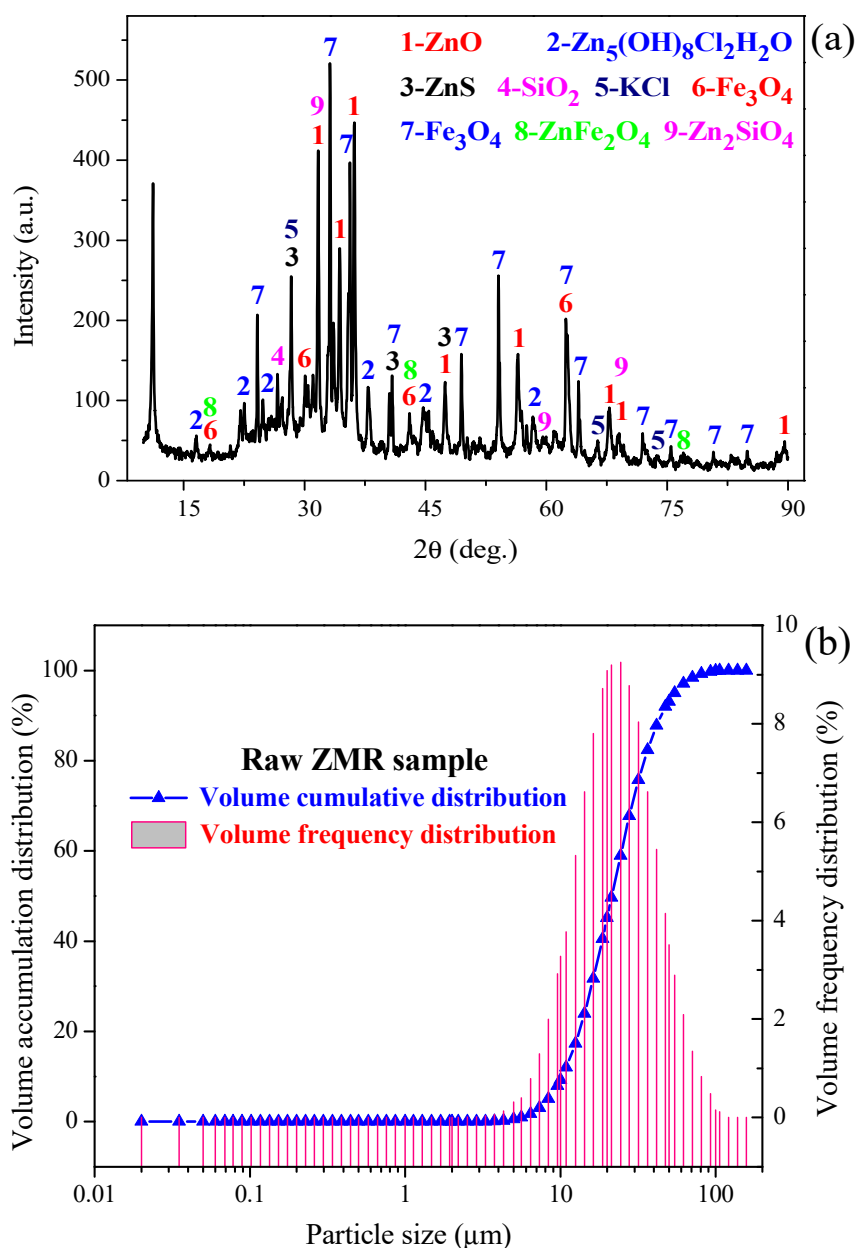


Figure 1. XRD pattern (a) and particle size distribution (b) of the raw ZMR sample.

Figure 2 illustrates the SEM image and EDS point analysis of the ZMR sample. As displayed in Figure 2, it is found that the bright particles (Point A) are mainly iron oxides, and the grey particles (Point B) are quartz. Furthermore, the valuable metal minerals and gangue components are embedded with each other to form an inclusion state in the raw material (see Figure 3), which the microstructure also indicates that it is difficult to recover Zn from ZMR.

2.2. Characterisation

The mineral phase of the ZMR samples before and after microwave calcium activation pretreatment and the leaching residue was determined by X-ray diffraction (TTR-III, Rigaku, Tokyo, Japan). The rotating anode powerful rotary target was used as the X-ray generator with the power of 18 kW, the voltage of 40 kV, the flow of 200 mA and CuK α ($\lambda = 1.54056 \text{ \AA}$) irradiation. Under the filtering of graphite monochromator with high reflection efficiency, the patterns of the samples were obtained at the scanning speed of $4^\circ/\text{min}$ in the range of $10\sim 90^\circ$ with $\theta\sim 2\theta$ step scanning. The microstructures of these samples were

analysed by the SEM (XL30ESEM-TMP, Philips, Amsterdam, The Netherlands) and EDS (EDS-Genesis, EDAX, Mahwah, NJ, USA) characterisations. The particle size characteristics of these samples were characterised by the laser particle size analyser (JL-1177, Shanghai Shuangxu Electronics Co.; Ltd., Shanghai, China).

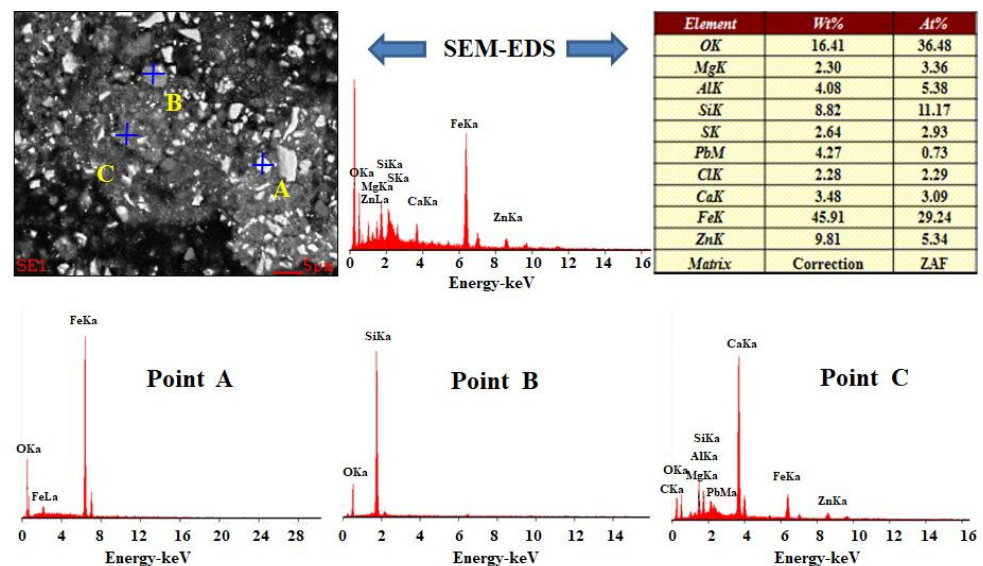


Figure 2. SEM image and EDS point analysis of the raw ZMR sample.

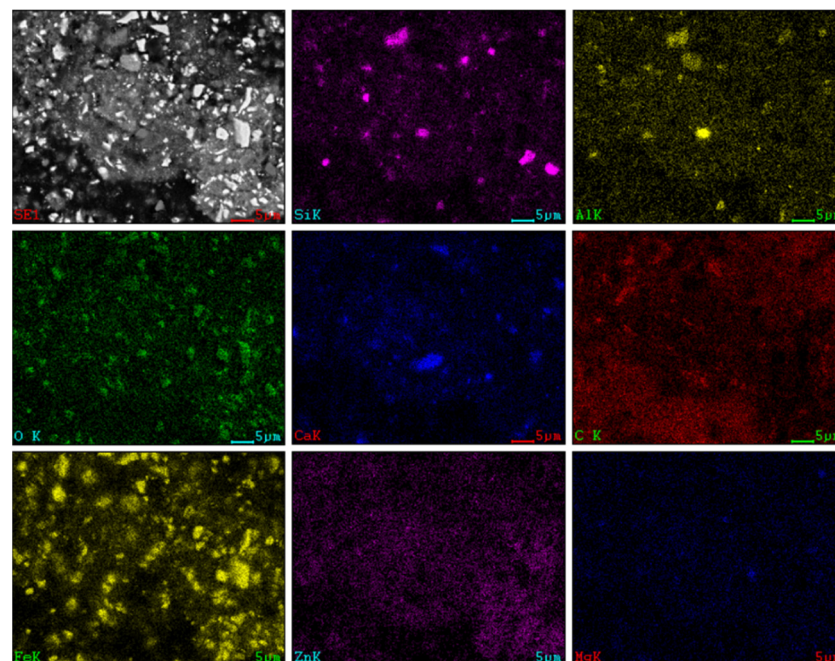


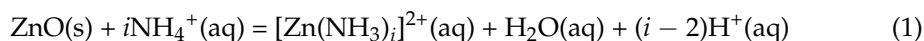
Figure 3. SEM image and EDS mapping analysis of the raw ZMR sample.

2.3. Procedure

The ZMR raw material was dried at 85 °C in a drying oven (DHG-9055A, Shanghai Shuangxu Electronics Co.; Ltd., Shanghai, China) to a constant weight. According to the previous basic theoretical research, the transformation of these refractory mineral phases can be realised by adding a proper amount of CaO under a certain roasting pretreatment temperature [15,26]. Therefore, before ammonium leaching, the dried ZMR sample was through microwave calcium activation pretreatment. During the pretreatment process, the roasting temperature varied among 100–600 °C, activation time varied among 0–50 min,

CaO addition varied among 0–30%. Meanwhile, a comparative experimental study of conventional roasting and microwave roasting was designed to explore the effects of activation temperature, CaO addition, and activation time on Zn leaching efficiency.

After calcium activation pretreatment, the roasted ZMR sample was leached using the freshly prepared ammonium acetate ($\text{NH}_3\text{-CH}_3\text{COONH}_4\text{-H}_2\text{O}$) leaching system in a 300 mL conical flask with stirring. The optimal leaching parameters included total ammonia concentration of 5 mol/L (including $c[\text{NH}_3]$ of 2.5 mol/L and $c[\text{CH}_3\text{COONH}_4]$ of 2.5 mol/L), a liquid-solid ratio of 5:1, leaching time of 60 min, leaching temperature of 25 °C, and stirring speed of 300 r/min, which the detailed investigation has been reported in the previous work [24]. In $\text{NH}_3\text{-CH}_3\text{COONH}_4\text{-H}_2\text{O}$ solutions, the dissolved zinc oxide (ZnO) can combine with ammonium ions and ammonia to form soluble $[\text{Zn}(\text{NH}_3)_i]^{2+}$ complexes, as shown in Equations (1) and (2) [24]:



After leaching, solids and liquids were separated, and the Zn concentration in the leaching solution was measured by EDTA titration method. The Zn leaching rate (η_{Zn} , %) is determined by Equation (3):

$$\eta_{\text{Zn}} = \frac{C_{\text{Zn}} \times V}{m \times W_{\text{Zn}}} \quad (3)$$

In Equation (3), C_{Zn} is the Zn concentration in the $\text{NH}_3\text{-CH}_3\text{COONH}_4\text{-H}_2\text{O}$ solution, g/L; V is the volume of the $\text{NH}_3\text{-CH}_3\text{COONH}_4\text{-H}_2\text{O}$ solution, L; m is the ZMR sample weight, g; W_{Zn} is the weight per cent of zinc in the ZMR sample, 24.74%.

3. Results and Discussion

3.1. Zinc Leaching Efficiency

Under the different pretreatments of conventional roasting and microwave roasting, the effects of activation temperature, CaO addition amount and activation time on Zn leaching efficiency were studied comparatively. Figure 4 shows the obtained results.

3.1.1. Effects of Activation Temperature

Figure 4a illustrates the effects of activation temperature on Zn leaching efficiency, by controlling the CaO addition of 25% and an activation time of 20 min. As displayed in Figure 4a, the Zn leaching rate was relatively low at low temperatures among 100 °C to 300 °C, with leaching efficiency values ranging from 84.19% to 85.68% under conventional roasting and from 87.69% to 90.28% under microwave roasting. With activation temperature increasing to 400 °C, the Zn leaching rate under microwave roasting reached 92.11%, which was 4.83% higher than that by conventional roasting. In addition, it is assumed that under the same temperature, the Zn leaching efficiencies under microwave roasting were all higher than that of conventional roasting. This finding was mainly attributed to the following two reasons. On the one hand, the distinctive selective and rapid heating merits of microwave heating induce thermal stress between useful minerals and gangues, causes cracks in the mineral particles, and increases the reaction area between useful minerals and the leaching solvent, thus facilitating the leaching reaction. On the other hand, the significant difference in the microwave absorption properties of useful minerals and gangues causes the microscopic non-uniform distribution of temperature in the multi-phase complicated system, which enhances the dissociation of useful minerals [43]. The above-formed non-equilibrium reaction conditions will promote the interfacial chemical reaction and realise the rapid transformation from complex refractory ores to easily leachable phases, thus achieving the improvement of Zn leaching efficiency. In addition, at temperatures higher than 450 °C, the Zn leaching rate obtained by microwave activation decreased slightly, which was mainly ascribed to that with the increase in temperature, the efficiency of ZnO reacting with Fe_2O_3 in raw materials to form ZnFe_2O_4 is higher than that of CaO

reacting with ZnFe_2O_4 to form ZnO . By studying the effect of CaO addition on the dielectric properties of ZMR at different temperatures, it is highlighted that the dielectric loss of the sample mixing with ZMR and CaO at $400\text{ }^\circ\text{C}$ evidently exceeds that at $500\text{ }^\circ\text{C}$, denoting that microwave energy could be better applied by controlling the activation temperature at $400\text{ }^\circ\text{C}$. Therefore, the subsequent activation experiment was carried out at $400\text{ }^\circ\text{C}$.

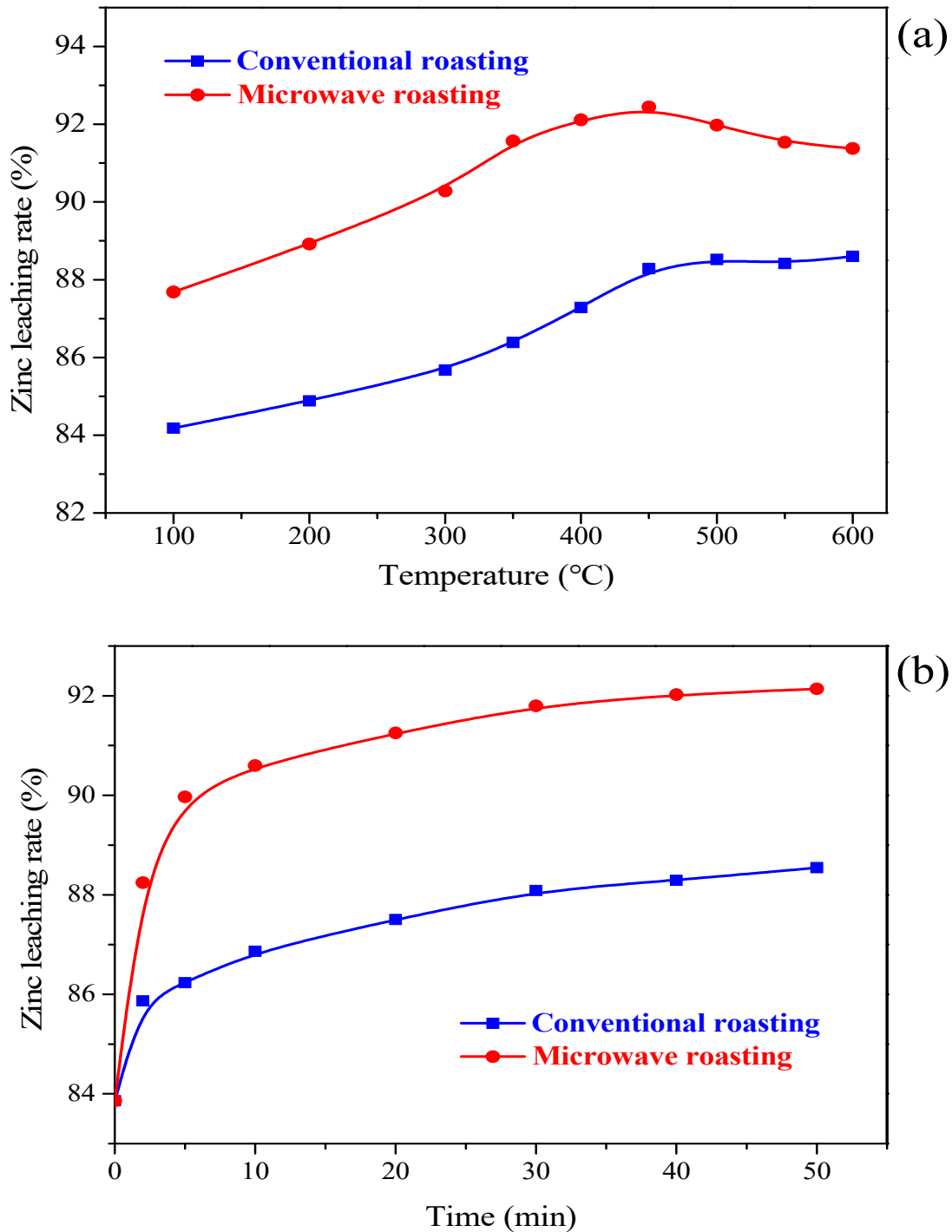


Figure 4. Cont.

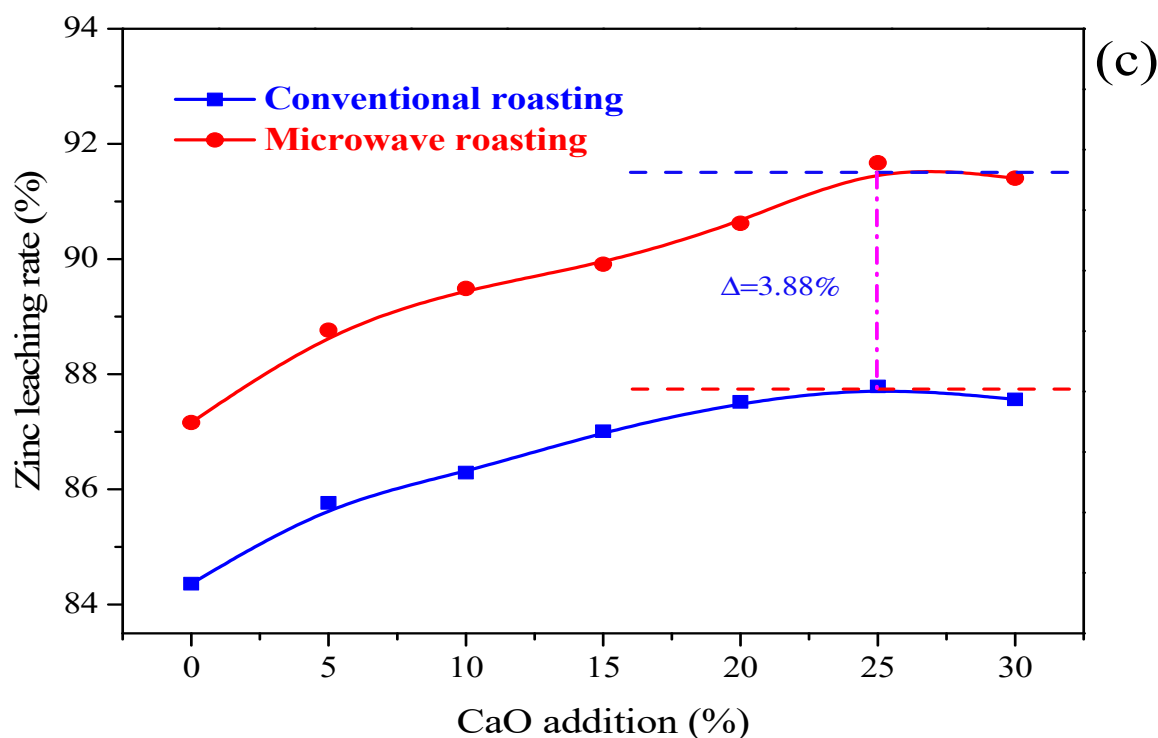


Figure 4. Effects of (a) activation temperature, (b) activation time, and (c) CaO addition to zinc leaching rate.

3.1.2. Effects of Activation Time

Figure 4b depicts the effects of activation time on Zn leaching rate, by controlling the CaO addition of 25% and an activation temperature of 400 °C. It can be seen from Figure 4b that the Zn leaching efficiency was markedly affected by the activation time, showing a good positive correlation. With an activation time of 20 min, the Zn leaching rate after the activation pretreatment under conventional roasting and microwave roasting was 88.55% and 91.25%, respectively. However, there was an absence of significant increase in the Zn leaching efficiency as the activation time prolonged to 50 min. The same finding was presented in Figure 4b that in contrast to conventional roasting process, microwave activation pretreatment could achieve high leaching efficiency in a shorter time. Considering the increase in energy consumption caused by the extension of microwave activation time, the microwave activation time of 20 min was preferred.

3.1.3. Effects of CaO Addition

Figure 4c presents the effects of CaO addition on Zn leaching rate, by controlling the activation temperature of 400 °C and an activation time of 20 min. As demonstrated in Figure 4c, it is summed that CaO addition has a pronounced influence on Zn leaching efficiency. A larger amount of CaO addition can promote the transformation of refractory phases in the ZMR to the easily leachable mineral phases, further realising the Zn leaching rate. The same finding also appeared between the relationship of CaO addition and Zn leaching rate, and the biggest difference value of Zn leaching rate between microwave roasting and conventional roasting arose under the CaO addition of 25%, with a value of 91.67% under microwave roasting and 87.79% under conventional roasting. As the CaO addition improved 30%, the Zn leaching efficiency tended to be balanced. In summary, the optimal CaO addition was determined at 25%.

3.2. XRD Characterisation

To clarify the mechanism of enhanced Zn leaching from ZMR via microwave calcium activation pretreatment, the effects of activation temperature on the phase transformation under microwave roasting and conventional roasting were investigated by XRD.

Figure 5a illustrates the XRD patterns of the ZMR sample under various microwave activation temperatures. As shown in Figure 5a, the main zinc phases in ZMR changed greatly after microwave activation pretreatment with CaO as the calcification agent. Zinc in the raw ZMR existed in the phases of zinc oxide (ZnO), zinc silicate (Zn_2SiO_4), zinc sulfide (ZnS), zinc ferrite (ZnFe_2O_4), and basic zinc chloride [$\text{Zn}_5(\text{OH})_8\text{Cl}_2 \cdot \text{H}_2\text{O}$]. After adding CaO as the calcification agent to pretreat ZMR by microwave roasting, the diffraction peak of $\text{Zn}_5(\text{OH})_8\text{Cl}_2 \cdot \text{H}_2\text{O}$ gradually decreased with temperature rising from 100 °C to 300 °C, and disappeared completely at 300 °C. As the temperature rose to 400 °C, ZnFe_2O_4 and Zn_2SiO_4 phases reacted with CaO, and were transformed into ZnO, $\text{Ca}_2\text{Fe}_2\text{O}_4$, $\text{Ca}_2\text{Fe}_2\text{O}_5$, CaFe_3O_5 , and Ca_2SiO_4 . The $\text{Ca}(\text{OH})_2$ phase completely disappeared at temperatures between 300 and 400 °C. The CaCO_3 phase arose at 400 °C, and the diffraction peak of ZnO was found to become stronger with temperature rising. The diffraction peaks of ZnO and the newly formed phases ($\text{Ca}_2\text{Fe}_2\text{O}_4$, $\text{Ca}_2\text{Fe}_2\text{O}_5$, CaFe_3O_5 , Ca_2SiO_4 , and CaCO_3) remained unchanged at temperatures exceeding 400 °C, denoting that the transformation of ZnFe_2O_4 and Zn_2SiO_4 into ZnO phase can be achieved at 400 °C. Besides, the intensity of the diffraction peaks of ZnS phase gradually weakened, but it did not disappear completely with the increase in temperature. Theoretically, the reaction of $\text{ZnS}(\text{s}) + \text{CaO}(\text{s}) = \text{ZnO}(\text{s}) + \text{CaS}(\text{s})$ could not occur at 400 °C, but the reaction of $2\text{ZnS}(\text{s}) + 3\text{O}_2(\text{g}) = 2\text{ZnO}(\text{s}) + 2\text{SO}_2(\text{g})$ could occur, indicating that part of ZnS was oxidized during the microwave calcium activation pretreatment process. In addition, Figure 5b displays the XRD patterns of the ZMR samples under various conventional roasting temperatures. As presented in Figure 5b, the complete transformation of zinc silicate (Zn_2SiO_4) and zinc ferrite (ZnFe_2O_4) required above 600 °C under conventional roasting pretreatment, in comparison with the same transformation occurred in the temperature range of 300–400 °C by microwave activation pretreatment. Meanwhile, it was found that the $\text{Ca}(\text{OH})_2$ decomposition temperature and CaCO_3 formation temperature under conventional roasting treatment were 600 °C and 400 °C, respectively. By contrast, under microwave activation pretreatment, $\text{Ca}(\text{OH})_2$ phase in raw ZMR material was decomposed completely at 400 °C, and CaCO_3 phase was formed at 300 °C. The findings denoted that microwave heating can shorten the process temperature compared with conventional heating, further reducing the production cost and energy consumption of the secondary zinc resource recovery industry. The excellent process advantage demonstrated by microwave heating is assigned to that microwave heating can realise selective heating based on the difference in the dielectric loss of various minerals, and the rapid dissociation and temperature increase in valuable minerals and gangue are achieved due to the complex compositions of ZMR under the action of microwave [44]. Therefore, the complete transformation temperature of mineral phases under microwave activation pretreatment is further reduced compared with the conventional pretreatment.

Figure 6 presents the XRD patterns of the microwave-activated ZMR sample at 400 °C and the leaching residue. It is concluded from Figure 6 that in the microwave-activated ZMR sample at 400 °C, ZnO and ZnS were the main phases. After leaching in $\text{NH}_3\text{-CH}_3\text{COONH}_4\text{-H}_2\text{O}$ solution, ferric oxide (Fe_2O_3), calcium carbonate (CaCO_3), calcium ferrite (including $\text{Ca}_2\text{Fe}_2\text{O}_5$, CaFe_3O_5 , and $\text{Ca}_2\text{Fe}_4\text{O}_7$), and calcium silicate (including CaSi_2O_5 , Ca_3SiO_5 , CaSiO_3 , and Ca_2SiO_4) appeared in the leaching residue, which is composed of Fe, Si, Ca, and O. Compared with the phase composition of the raw ZMR (Figure 1), it is summed that the intensities of the diffraction peak of ZnO and ZnS phases became stronger after microwave calcium activation pretreatment. It can also be observed from Figure 6b that the refractory mineral phases (including Zn_2SiO_4 and ZnFe_2O_4) disappeared and were successfully calcified and transformed into the easy-to-handle mineral phases, like calcium ferrite (including $\text{Ca}_2\text{Fe}_2\text{O}_5$, CaFe_3O_5 , and $\text{Ca}_2\text{Fe}_4\text{O}_7$) and calcium silicate (including CaSi_2O_5 , Ca_3SiO_5 , CaSiO_3 , and Ca_2SiO_4). Combining with the obtained Zn leaching efficiency in Figure 4, the phase change of ZMR samples before and after microwave calcium activation pretreatment verifies that CaO activation is an efficient pretreatment approach to ameliorate the leaching efficiency of zinc from ZMR.

3.3. SEM-EDS Characterisation

To further evaluate the advantages of microwave activation pretreatment on the enhanced zinc leaching from ZMR, SEM-EDS characterisations were utilised to observe the microstructures change of the ZMR samples before and after microwave activation pretreatment and the leaching residue.

3.3.1. SEM Characterisation

Figure 7 presents the corresponding SEM images. As displayed in Figure 7, obvious cracks arose in the samples pretreated by microwave activation and the subsequent leaching residue, in contrast with no crack was observed in the raw ZMR and the ZMR sample pretreated by conventional activation. As exhibited in Figure 7a,b, the morphology of the sample before and after conventional roasting pretreatment was almost the same, and the agglomeration was more obvious. This phenomenon denoted the unique heating characteristics of microwave heating. During the microwave activation pretreatment process, the microwave-absorbing properties of useful minerals and gangues present huge differences, leading to the uneven heat distribution in this multi-element and multi-phase complex ore system. The unique selective heating mode of microwave generates thermal stress between useful minerals and gangues, which causes the mineral inclusion particles to crack, strengthens the dissociation of useful minerals, achieving the dissociation effect that is difficult to achieve by conventional methods [43,44]. Meanwhile, the increased reaction area at the interface of useful minerals and accelerated diffusion efficiency also accompanies with the generation of crack, further contributing to the enhanced leaching of zinc from ZMR.

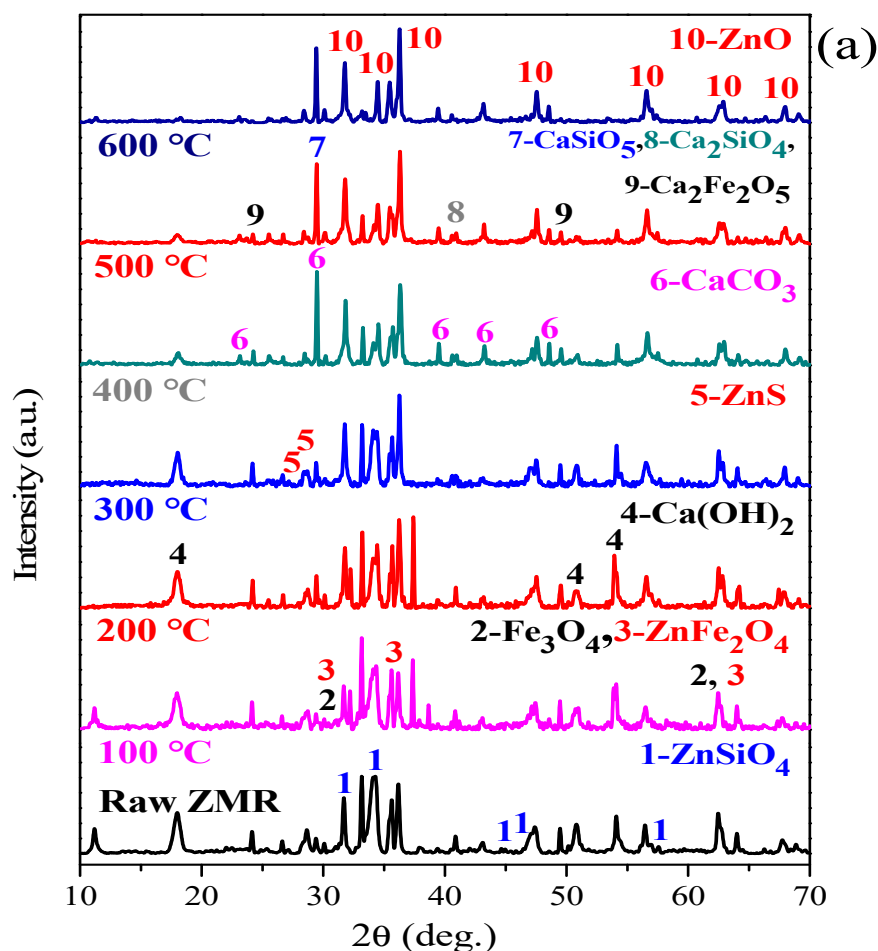


Figure 5. Cont.

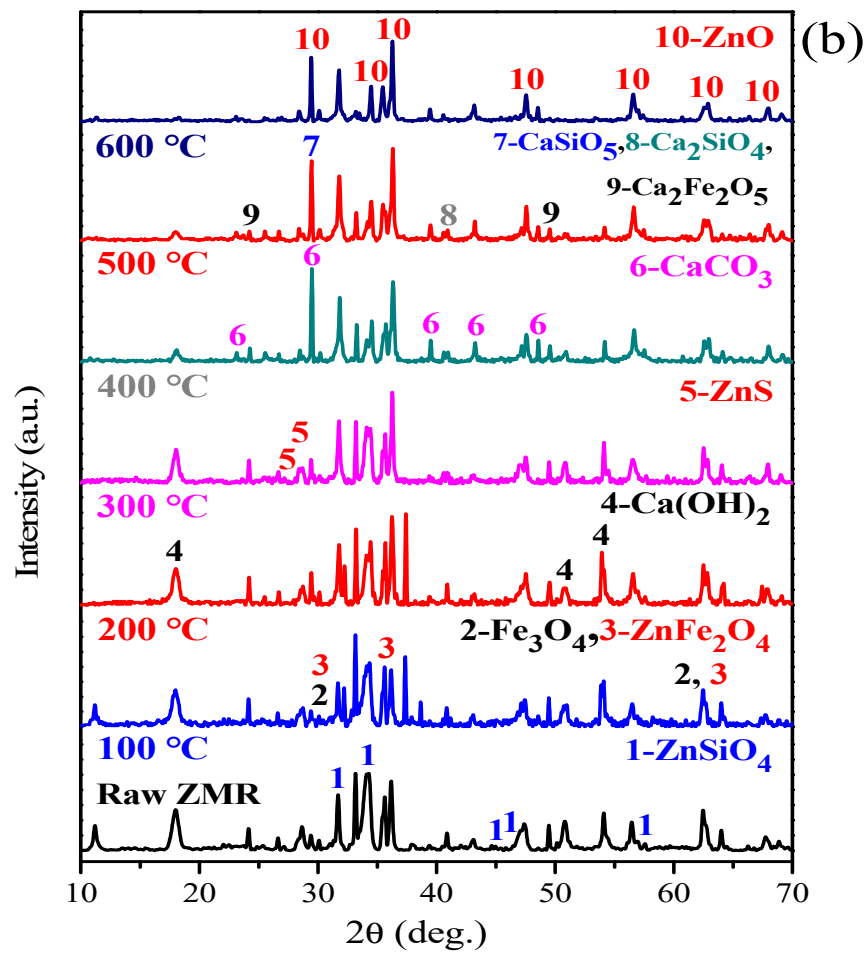


Figure 5. XRD patterns of the ZMR sample under (a) various microwave activation temperatures and (b) various conventional roasting temperatures.

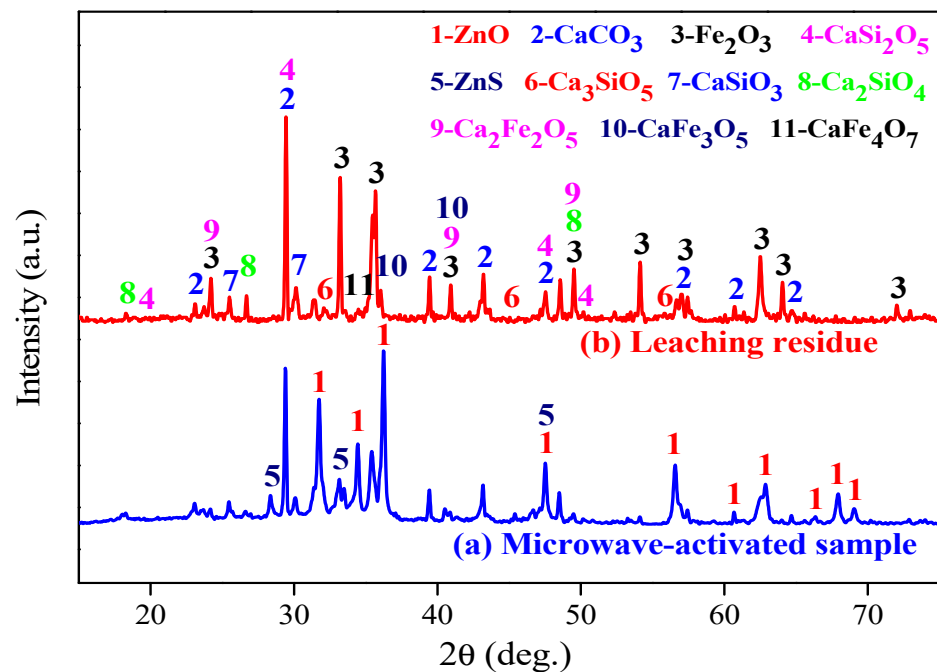


Figure 6. XRD patterns of (a) the microwave-activated ZMR sample and (b) the leaching residue.

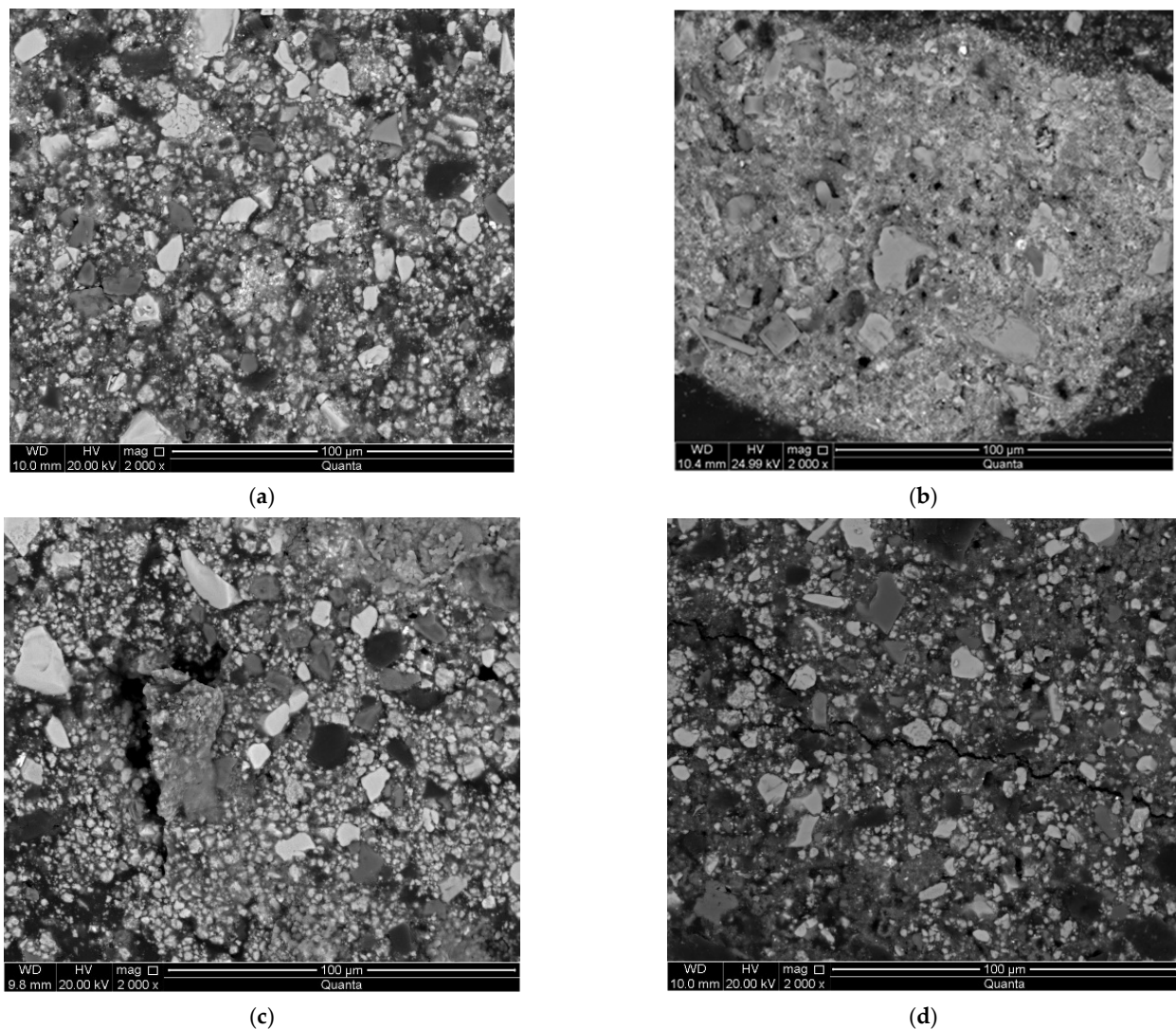


Figure 7. SEM images of the ZMR samples (a) before pretreatment and (b) after conventional pretreatment and (c) microwave pretreatment and (d) the leaching residue.

3.3.2. EDS Characterisation

Figure 8 exhibits the corresponding EDS point analysis results of the ZMR samples before and after microwave activation pretreatment, and the leaching residue. As shown in Figure 8B, there were mainly three morphologies in the microwave-activated ZMR sample: (1) point (a), bright white cluster particles; (2) point (b), amorphous grey fine particles; (3) point (c), grey bulk particle. A similar finding was observed from Figure 8A where the three morphologies were embedded and wrapped. The grey fine particles were distributed over most of the region. Moreover, the difference between Figure 8A,B was demonstrated by that the bright white cluster particles were exposed after microwave activation pretreatment. In more detail, it was summarised that the main phase composition of the cluster particles was ZnO phase (Figure 8A), the amorphous grey fine particles were mainly the agglomeration area of Zn, and the grey bulk particles were mainly iron oxides. In addition, as showed in Figure 8C, there were also mainly three morphologies in the leaching residue: (a) bright grey particles; (b) amorphous dark grey fine particles; (c) dark black particles. As illustrated in Figure 8B, long cracks arose among the three types of morphology particles after the microwave activation pretreatment. The EDS analysis of point (a) indicated that the bright grey particles were mainly iron oxides with a small amount of Au, which is ascribed to the gold spraying on the sample surface increases its conductivity during the

preparation of the characterised sample. The EDS analysis of point (b) indicated that the amorphous dark grey fine particles were composed of Si, O, Ca, Fe, Al, S, Cl, and Zn, and the presence of a large amount of Cr in this area was due to the addition of polishing agent containing mainly chromium trioxide when polishing the surface of the embedded powder sample. The EDS analysis of point (c) denoted that dark black particles were mainly gangue minerals. Furthermore, by comparing the Zn content in the amorphous grey fine particles in Figure 8C, it is found that the Zn content in the leaching residue is significantly reduced, with the weight percentage of 67.31% for the raw ZMR, 41.79% for the microwave-activated ZMR sample, and 3.66% for the leaching residue. Meanwhile, the Fe content is also significantly reduced, with the weight percentage of 6.70% for the raw ZMR, 4.74% for the microwave-activated ZMR sample, and 3.72% for the leaching residue.

EDS line scanning analysis was utilised to further clarify the phase changes of ZMR during microwave activation pretreatment process and the leaching process, and the corresponding results are provided in Figure 9. Specifically, combined with the analysis results in Figure 7, it can be summarised that the phase of Zn in the raw ZMR sample before activation pretreatment had not changed. It mainly existed in the form of ZnO, Zn₂SiO₄ and ZnS, and ZnFe₂O₄ (see Figure 9A). Besides, combined with the analysis results in Figure 9, it can be surmised that after adding CaO as the activation agent, Zn₂SiO₄ and ZnFe₂O₄ were transformed into ZnO, Ca₂Fe₂O₅, and Ca₂SiO₄ (see Figure 9B). Meanwhile, ZnS still existed in the sample after the microwave activation, matched to the XRD findings (Figure 5). Furthermore, combined with the analysis results in Figure 9, it is summed that the peaks of ZnO phase disappeared completely after NH₃-CH₃CONH₄-H₂O leaching. The leaching residue mainly contained the easily leachable phases such as Ca₂Fe₂O₅, Ca₂SiO₄ and ZnS (see Figure 9C). In summary, the findings obtained from SEM-EDS analysis were matched to the XRD analysis results.

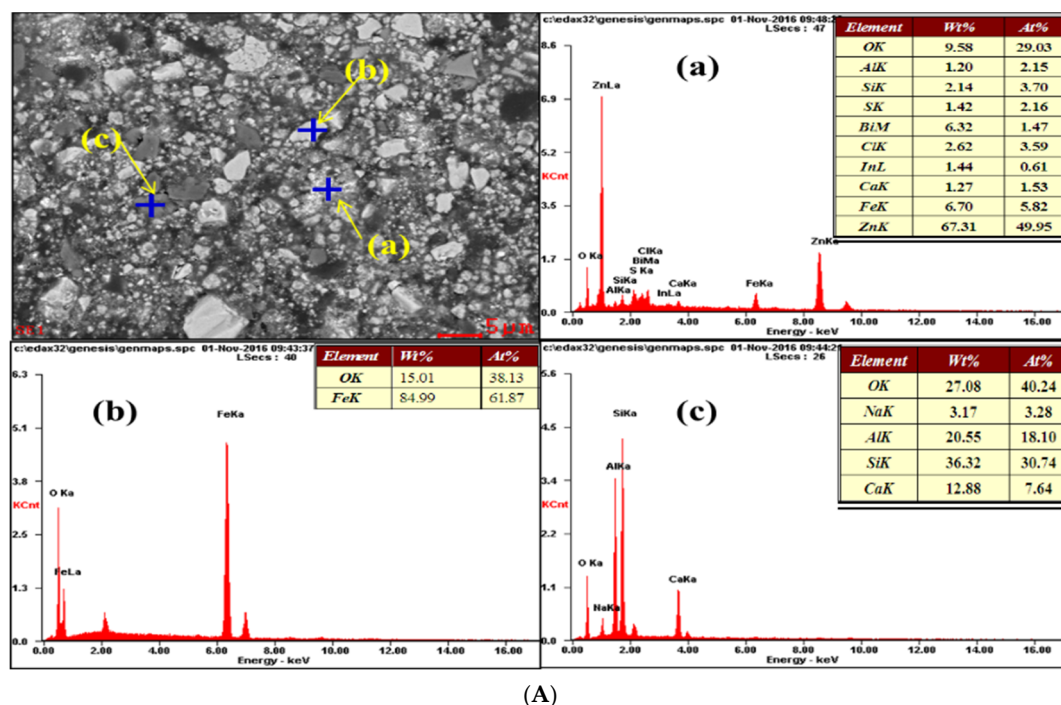


Figure 8. Cont.

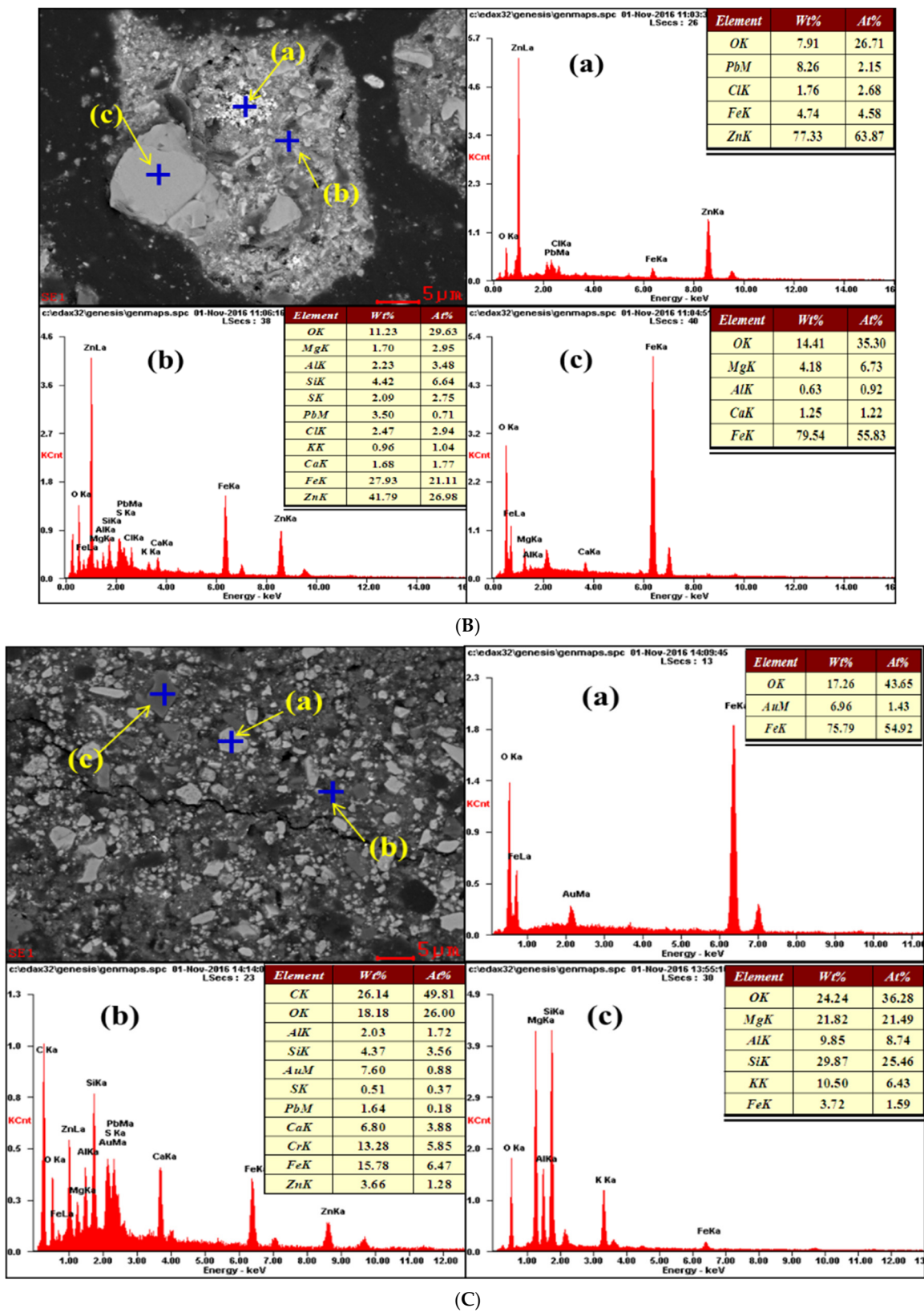


Figure 8. EDS point analysis of the raw ZMR sample (A), the microwave-activated ZMR sample (B), and the leaching residue (C).

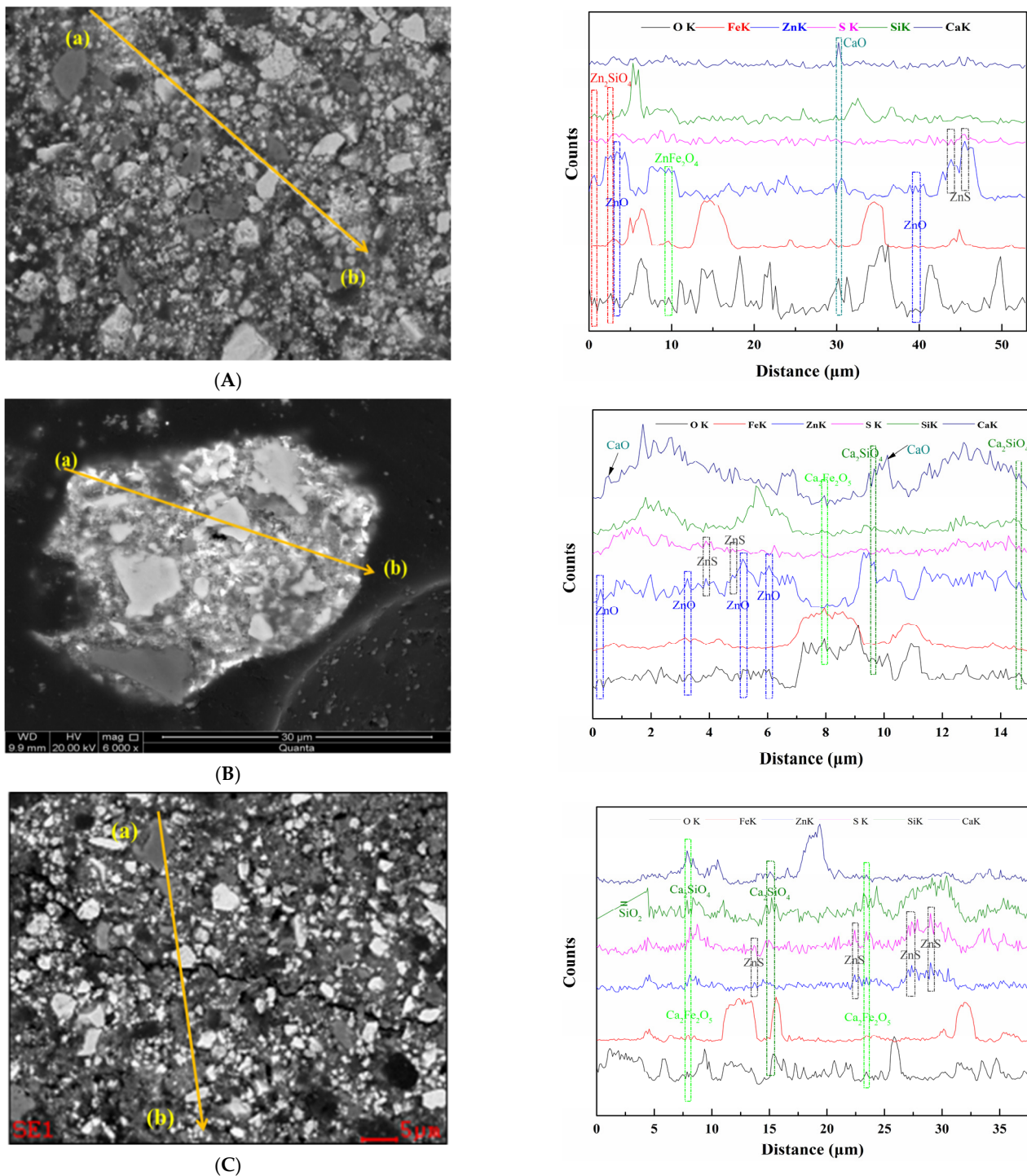


Figure 9. EDS line scanning of the raw ZMR sample (A), the microwave-activated ZMR sample (B), and the leaching residue (C).

3.4. Mechanism of Enhanced Leaching Zn by Microwave Calcium Activation Pretreatment

Figure 10 presents the particle size distribution characteristics of the ZMR samples after microwave activation pretreatment and the leaching residue. Table 2 lists the detailed particle size parameters. As presented in Figure 10 and Table 2, compared with the raw ZMR sample, the parameter values of D_{10} , D_{50} , D_{90} and D_{98} gradually increased for the ZMR samples after microwave activation pretreatment and the leaching residue, altogether with the area average particle size, the volume average particle size and the corresponding surface area to volume ratio. The increase in these parameters may be attributed to the disappearance of the ZnO phase that is mainly distributed in fine particles after leaching

and the phase transformation of the refractory mineral phases into the easily leachable mineral phases. In addition, in order to investigate the leaching of other harmful impurity elements in ZMR with zinc, the chemical element content of Zn, Pb, Fe, Ca, and Si in the leaching solution at 25 °C was determined, and the content in the leaching solution was determined at 41.15 g/L (Zn), 0.0094 g/L (Pb), 0.0208 g/L (Fe), 0.66 g/L (Ca), 0.094 mg/L (Si), respectively. The analysis results indicated that the $\text{NH}_3\text{-CH}_3\text{COONH}_4\text{-H}_2\text{O}$ system can selectively leach Zn without leaching metal and alkaline gangue impurities like Pb, Fe, Ca, Si, and etc. The relevant data have been published in the work [25].

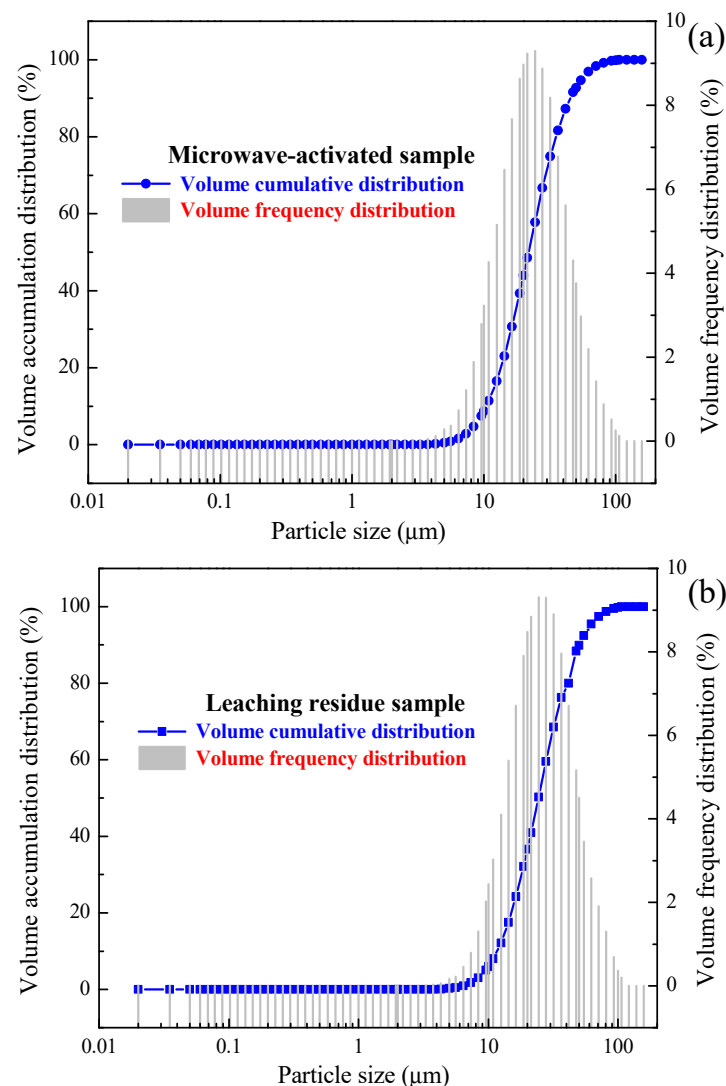


Figure 10. Particle size distribution of the ZMR samples (a) after microwave activation pretreatment and (b) the leaching residue.

Table 2. Particle size parameters of the ZMR samples (A) before and (B) after microwave activation pretreatment and (C) the leaching residue.

Samples	D ₁₀ (μm)	D ₅₀ (μm)	D ₉₀ (μm)	D ₉₈ (μm)	Volume Average Particle Size (μm)	Area Average Particle Size (μm)	Surface Area to Volume Ratio (m ² /cm ³)
A	10.26	21.42	44.67	68.15	23.40	19.40	2.48
B	10.44	21.80	45.33	68.93	23.78	19.74	2.60
C	11.68	24.27	50.17	75.21	26.35	22.03	2.73

In summary, combining with the above analysis results obtained from Zn leaching efficiency, XRD characterisation, SEM-EDS characterisation, and particle size analysis, the

mechanism of enhanced Zn leaching from zinc-containing metallurgical residues (ZMR) by microwave activation pretreatment can be deduced. Under the activation action of CaO, the refractory mineral phases (including Zn_2SiO_4 and $ZnFe_2O_4$) were transformed into the easily leachable mineral phases, like ZnO phase, calcium ferrite (including $Ca_2Fe_2O_5$, $CaFe_3O_5$, and $Ca_2Fe_4O_7$) and calcium silicate (including $CaSi_2O_5$, Ca_3SiO_5 , $CaSiO_3$, and Ca_2SiO_4). Meanwhile, the unique selective heating characteristic of microwave heating induces thermal stress formed between the valuable minerals and gangues, and the thermal stress renders the mineral inclusion particles dissociate to long and significant cracks. Meanwhile, the cracks contribute to increasing the reaction area and accelerating the diffusion efficiency, further promoting the improvement of leaching efficiency of zinc from ZMR.

4. Conclusions

In this work, an enhanced Zn leaching approach from zinc-containing metallurgical residues was proposed, by introducing a microwave heating approach into the CaO activation pretreatment process to realise the conversion of refractory ore phases into the easily leachable ore phase. The main findings were depicted as follows:

- (1) The influences of CaO addition, activation temperature and activation time on the Zn leaching efficiency were studied in the $NH_3-CH_3COONH_4-H_2O$ system. The preferred microwave calcium activation pretreatment parameters were determined with a zinc leaching rate of 91.67% under a roasting temperature of 400 °C, the activation time of 20 min, and a CaO addition of 25%. Meanwhile, the Zn leaching efficiencies under microwave roasting were all higher than those by conventional roasting.
- (2) XRD and SEM-EDS analysis indicated that under microwave calcification pretreatment, the refractory mineral zinc silicate (Zn_2SiO_4) and zinc ferrite ($ZnFe_2O_4$) were converted into the easily leachable mineral phases, like zinc oxide, calcium ferrite, and calcium silicate. The diffraction peak of ZnS was weakened after microwave activation, thus increasing the content of easily leachable mineral phase ZnO and promoting the leaching of zinc. Moreover, microwave heating can shorten the process temperature, manifested by the $Ca(OH)_2$ decomposition temperature and $CaCO_3$ formation temperature decreased by 200 °C and 100 °C, respectively. Furthermore, the selective heating characteristics of microwave heating render the mineral inclusion particles dissociated into cracks, which increases the reaction area and the diffusion efficiency, further enhancing the leaching process of zinc from zinc-containing metallurgical residues.

Author Contributions: Conceptualization, A.M., G.C., K.L., M.O. and X.Z.; methodology, M.O., A.M. and G.C.; formal analysis, G.C., L.G. and A.M.; investigation, A.M., M.O., G.C. and K.L.; resources, G.C.; writing—original draft preparation, A.M.; writing—review and editing, M.O., G.C., K.L. and A.M.; supervision, G.C.; funding acquisition, A.M. All authors have read and agreed to the published version of the manuscript.

Funding: This work was supported by the Guizhou Province Science and Technology Project (No. [2019]1444, No. [2020]2001), the Guizhou Provincial Colleges and Universities Science and Technology Talent Project (KY [2020]124), the Science and Technology Innovation Group of Liupanshui Normal University (LPSSYKJTD201801), the Key cultivation disciplines of Liupanshui Normal University (LPSSYZDXK202001).

Institutional Review Board Statement: Not applicable.

Informed Consent Statement: Not applicable.

Data Availability Statement: The data presented in this study are available on request from the corresponding author. The data are not publicly available due to technical or time limitations.

Acknowledgments: The authors acknowledge the financial supports to carry out this work.

Conflicts of Interest: The authors declare no conflict of interest.

References

1. Zhu, X.L.; Xu, C.Y.; Tang, J.; Hua, Y.X.; Zhang, Q.B.; Liu, H.; Wang, X.; Huang, M.T. Selective recovery of zinc from zinc oxide dust using choline chloride based deep eutectic solvents. *Trans. Nonferr. Met. Soc.* **2019**, *29*, 2222–2228. [[CrossRef](#)]
2. Wang, J.; Huang, Q.F.; Li, T.; Xin, B.P.; Chen, S.; Guo, X.M.; Liu, C.H.; Li, Y.P. Bioleaching mechanism of Zn, Pb, In, Ag, Cd and As from Pb/Zn smelting slag by autotrophic bacteria. *J. Environ. Manag.* **2015**, *159*, 11–17. [[CrossRef](#)]
3. Abkhoshk, E.; Jorjani, E.; Al-Harashseh, M.S.; Rashchi, F.; Naazeri, M. Review of the hydrometallurgical processing of non-sulfide zinc ores. *Hydrometallurgy* **2014**, *149*, 153–167. [[CrossRef](#)]
4. Ejtemaei, M.; Gharabaghi, M.; Irannajad, M. A review of zinc oxide mineral beneficiation using flotation method. *Adv. Colloid. Interface Sci.* **2014**, *206*, 68–78. [[CrossRef](#)]
5. Jaafar, I.; Griffiths, A.J.; Hopkins, A.C.; Steer, J.M.; Griffiths, M.H.; Sapsford, D.J. An evaluation of chlorination for the removal of zinc from steelmaking dusts. *Miner. Eng.* **2011**, *24*, 1028–1030. [[CrossRef](#)]
6. Oustadakis, P.; Tsakiridis, P.E.; Katsiapi, A.; Agatzini-Leonardou, S. Hydrometallurgical process for zinc recovery from electric arc furnace dust (EAFD): Part I: Characterisation and leaching by diluted sulphuric acid. *J. Hazard. Mater.* **2010**, *179*, 1–7. [[CrossRef](#)] [[PubMed](#)]
7. Antrekowitsch, J.; Steinlechner, S. The recycling of heavy-metal containing wastes: Mass balances and economical estimations. *JOM* **2011**, *63*, 68–72. [[CrossRef](#)]
8. Lima, L.R.P.D.A.; Bernardes, L.A. Characterisation of the lead smelter slag in Santo Amaro, Bahia, Brazil. *J. Hazard. Mater.* **2011**, *189*, 692–699. [[CrossRef](#)] [[PubMed](#)]
9. Yina, N.H.; Sivryb, Y.; Guyotc, F.; Lensd, P.N.L.; Hullebuscha, E.D.V. Evaluation on chemical stability of lead blast furnace (LBF) and imperial smelting furnace (ISF) slags. *J. Environ. Manag.* **2016**, *180*, 310–323. [[CrossRef](#)] [[PubMed](#)]
10. Hu, H.P.; Deng, Q.F.; Li, C.; Xie, Y.; Dong, Z.Q.; Zhang, W. The recovery of Zn and Pb and the manufacture of lightweight bricks from zinc smelting slag and clay. *J. Hazard. Mater.* **2014**, *271*, 220–227. [[CrossRef](#)] [[PubMed](#)]
11. Li, M.; Peng, B.; Chai, L.Y.; Peng, N.; Yan, H.; Hou, D.K. Recovery of iron from zinc leaching residue by selective reduction roasting with carbon. *J. Hazard. Mater.* **2012**, *237–238*, 323–330. [[CrossRef](#)]
12. Sun, Y.; Shen, X.Y.; Zhai, Y.C. Thermodynamics and kinetics of extracting zinc from zinc oxide ore by ammonium sulfate roasting method. *Int. J. Miner. Metall. Mater.* **2015**, *22*, 467–475. [[CrossRef](#)]
13. Havlik, T.; Souza, B.V.; Bernardes, A.M.; Schneider, I.A.H.; Miskufova, A. Hydrometallurgical processing of carbon steel EAF dust. *J. Hazard. Mater.* **2006**, *135*, 311–318. [[CrossRef](#)] [[PubMed](#)]
14. Miki, T.; Chairaksa-Fujimoto, R.; Maruyama, K.; Nagasaka, T. Hydrometallurgical extraction of zinc from CaO treated EAF dust in ammonium chloride solution. *J. Hazard. Mater.* **2016**, *302*, 90–96. [[CrossRef](#)] [[PubMed](#)]
15. Chairaksa-Fujimoto, R.; Maruyama, K.; Miki, T.; Nagasaka, T. The selective alkaline leaching of zinc oxide from Electric Arc Furnace dust pre-treated with calcium oxide. *Hydrometallurgy* **2016**, *159*, 120–125. [[CrossRef](#)]
16. Soria-Aguilar, M.d.J.; Davila-Pulido, G.I.; Carrillo-Pedroza, F.R.; Gonzalez-Ibarra, A.A.; Picazo-Rodriguez, N.; Lopez-Saucedo, F.d.J.; Ramos-Cano, J. Oxidative leaching of zinc and alkalis from iron blast furnace sludge. *Metals* **2019**, *9*, 1015. [[CrossRef](#)]
17. Tsakiridis, P.E.; Oustadakis, P.; Katsiapi, A.; Agatzini-Leonardou, S. Hydrometallurgical process for zinc recovery from electric arc furnace dust (EAFD). Part II: Downstream processing and zinc recovery by electrowinning. *J. Hazard. Mater.* **2010**, *179*, 8–14. [[CrossRef](#)]
18. Picazo-Rodríguez, N.G.; Soria-Aguilar, M.d.J.; Martínez-Luévanos, A.; Almaguer-Guzmán, I.; Chaidez-Félix, J.; Carrillo-Pedroza, F.R. Direct acid leaching of sphalerite: An approach comparative and kinetics analysis. *Minerals* **2020**, *10*, 359. [[CrossRef](#)]
19. Montenegro, V.; Agatzini-Leonardou, S.; Oustadakis, P.; Tsakiridis, P. Hydrometallurgical treatment of EAF dust by direct sulphuric acid leaching at atmospheric pressure. *Waste Biomass Valoriz.* **2016**, *7*, 1531–1548. [[CrossRef](#)]
20. Zhao, Y.C.; Stanforth, R. Extraction of zinc from zinc ferrites by fusion with caustic soda. *Miner. Eng.* **2000**, *13*, 1417–1421.
21. Shen, X.Y.; Shao, H.M.; Gu, H.M.; Chen, B.; Ma, P.H. Reaction mechanism of roasting Zn_2SiO_4 using NaOH. *Trans. Nonferr. Met. Soc.* **2018**, *28*, 1878–1886. [[CrossRef](#)]
22. Liu, Z.Y.; Zhang, J.X.; Liu, Z.H.; Li, Q.H. Thermodynamics of metal ion complex formation in the Zn_2SiO_4 - NH_3 - $(NH_4)_2SO_4$ - H_2O system (I): Analysis of the Zn(II) complex equilibrium Hydrometallurgy 2018, *178*, 12–18. *Hydrometallurgy* **2018**, *178*, 12–18. [[CrossRef](#)]
23. Yang, S.H.; Li, H.; Sun, Y.W.; Chen, Y.M.; Tang, C.B.; He, J. Leaching kinetics of zinc silicate in ammonium chloride solution. *Trans. Nonferr. Met. Soc.* **2016**, *26*, 1688–1695. [[CrossRef](#)]
24. Ma, A.Y.; Zheng, X.M.; Li, S.; Wang, Y.H.; Zhu, S. Zinc recovery from metallurgical residues by coordination leaching in NH_3 - CH_3COONH_4 - H_2O system. *R. Soc. Open Sci.* **2018**, *5*, 180660. [[CrossRef](#)]
25. Liu, Z.Y.; Liu, Z.H.; Li, Q.H.; Cao, Z.Y.; Yang, T.Z. Dissolution behavior of willemite in the $(NH_4)_2SO_4$ - NH_3 - H_2O system. *Hydrometallurgy* **2012**, *125–126*, 50–54. [[CrossRef](#)]
26. Chairaksa-Fujimoto, R.; Inoue, Y.; Umeda, N.; Itoh, S.; Nagasak, T. New pyrometallurgical process of EAF dust treatment with CaO addition. *Int. J. Miner. Metall. Mater.* **2015**, *22*, 788–797. [[CrossRef](#)]
27. Li, K.Q.; Chen, J.; Peng, J.H.; Ruan, R.; Srinivasakannan, C.; Chen, G. Pilot-scale study on enhanced carbothermal reduction of low-grade pyrolusite using microwave heating. *Powder Technol.* **2020**, *360*, 846–854. [[CrossRef](#)]
28. Li, K.Q.; Jiang, Q.; Chen, J.; Peng, J.H.; Li, X.P.; Koppala, S.; Omran, M.; Chen, G. The controlled preparation and stability mechanism of partially stabilized zirconia by microwave intensification. *Ceram. Int.* **2020**, *46*, 7523–7530. [[CrossRef](#)]

29. Wei, Y.Q.; Peng, J.H.; Zhang, L.B.; Ju, S.H.; Xia, Y.; Zheng, Q.; Wang, Y.J. Dechlorination of zinc dross by microwave roasting. *J. Cent. South Univ.* **2014**, *21*, 2627–2632. [[CrossRef](#)]
30. Yang, K.; Li, S.W.; Zhang, L.B.; Peng, J.H.; Chen, W.H.; Xie, F.; Ma, A.Y. Microwave roasting and leaching of an oxide-sulphide zinc ore. *Hydrometallurgy* **2016**, *166*, 243–251. [[CrossRef](#)]
31. Omran, M.; Fabritius, T.; Heikkinen, E.-P.; Vuolio, T.; Yu, Y.; Chen, G.; Kacar, Y. Microwave catalyzed carbothermic reduction of zinc oxide and zinc ferrite: Effect of microwave energy on the reaction activation energy. *RSC Adv.* **2020**, *10*, 23959–23968. [[CrossRef](#)]
32. Zhang, M.Y.; Gao, L.; Kang, J.; Omran, M.; Chen, G. Stability optimisation of CaO-doped partially stabilised zirconia by microwave sintering. *Ceram. Int.* **2019**, *45*, 23278–23282. [[CrossRef](#)]
33. Omran, M.; Fabritius, T.; Heikkinen, E.-P.; Chen, G. Dielectric properties and carbothermic reduction of zinc oxide and zinc ferrite by microwave heating. *R. Soc. Open Sci.* **2017**, *4*, 170710. [[CrossRef](#)]
34. Chen, G.; Jiang, Q.; Omran, M.; Li, K.Q.; He, A.X.; Peng, J.H. Simultaneous removal of Cr(III) and V(V) and enhanced synthesis of high-grade rutile TiO₂ based on sodium carbonate decomposition. *J. Hazard. Mater.* **2020**, *388*, 12203. [[CrossRef](#)]
35. Li, K.Q.; Jiang, Q.; Chen, G.; Gao, L.; Peng, J.H.; Chen, Q.; Koppala, S.; Omran, M.; Chen, J. Kinetics characteristics and microwave reduction behavior of walnut shell-pyrolusite blends. *Bioresour. Technol.* **2021**, *319*, 124172. [[CrossRef](#)]
36. Li, K.Q.; Jiang, Q.; Gao, L.; Chen, J.; Peng, J.H.; Koppala, S.; Omran, M.; Chen, G. Investigations on the microwave absorption properties and thermal behavior of vanadium slag: Improvement in microwave oxidation roasting for recycling vanadium and chromium. *J. Hazard. Mater.* **2020**, *395*, 122698. [[CrossRef](#)] [[PubMed](#)]
37. Li, K.Q.; Chen, J.; Peng, J.H.; Ruan, R.; Omran, M.; Chen, G. Dielectric properties and thermal behavior of electrolytic manganese anode mud in microwave field. *J. Hazard. Mater.* **2020**, *381*, 121227. [[CrossRef](#)]
38. Omran, M.; Fabritius, T.; Heikkinen, E.-P. Selective zinc removal from electric arc furnace (EAF) dust by using microwave heating. *J. Sustain. Metall.* **2019**, *5*, 331–340. [[CrossRef](#)]
39. Chen, G.; Li, K.Q.; Omran, M.; Jiang, Q.; Li, X.P.; Peng, J.H.; Chen, J. Microstructure and enhanced volume density properties of FeMn78C8.0 alloy prepared via a cleaner microwave sintering approach. *J. Clean. Prod.* **2020**, *262*, 121364. [[CrossRef](#)]
40. Al-Harashsheh, M.; Kingman, S.W. Microwave-assisted leaching—a review. *Hydrometallurgy* **2004**, *73*, 189–203. [[CrossRef](#)]
41. Ling, Y.Q.; Li, Q.N.; Zheng, H.W.; Omran, M.; Gao, L.; Chen, J.; Chen, G. Optimisation on the stability of CaO-doped partially stabilised zirconia by microwave heating. *Ceram. Int.* **2021**, *47*, 8067–8080. [[CrossRef](#)]
42. Kang, J.X.; Omran, M.; Zhang, M.Y.; Pu, J.; He, L.; Ruan, R.S.; Peng, J.H.; Chen, G. Synthesis of rutile TiO₂ powder by microwave-enhanced roasting followed by hydrochloric acid leaching. *Adv. Powder Technol.* **2020**, *31*, 1140–1147. [[CrossRef](#)]
43. Sahoo, B.K.; De, S.; Meikap, B.C. Improvement of grinding characteristics of Indian coal by microwave pre-treatment. *Fuel Process. Technol.* **2011**, *92*, 1920–1928. [[CrossRef](#)]
44. Li, K.Q.; Chen, J.; Peng, J.H.; Omran, M.; Chen, G. Efficient improvement for dissociation behavior and thermal decomposition of manganese ore by microwave calcination. *J. Clean. Prod.* **2020**, *260*, 121074. [[CrossRef](#)]